Multi-Task Learning via Time-Aware Neural ODE

Feiyang Ye[1,2,3,4], **Xuehao Wang** [1], **Yu Zhang** [1,5 *], **Ivor W. Tsang**[2,3,4]
[1] Department of Computer Science and Engineering, Southern University of Science and Technology
[2] Australian Artificial Intelligence Institute, University of Technology Sydney
[3] Centre for Frontier AI Research, A*STAR
[4] Institute of High Performance Computing, A*STAR
[5] Peng Cheng Laboratory
{yefeiyang123, xuehaowangfi, yu.zhang.ust}@gmail.com
ivor.tsang@uts.edu.au

Abstract

Multi-Task Learning (MTL) is a well-established paradigm for learning shared models for a diverse set of tasks. Moreover, MTL improves data efficiency by jointly training all tasks simultaneously. However, directly optimizing the losses of all the tasks may lead to imbalanced performance on all the tasks due to the competition among tasks for the shared parameters in MTL models. Many MTL methods try to mitigate this problem by dynamically weighting task losses or manipulating task gradients. Different from existing studies, in this paper, we propose a Neural Ordinal diffeRential equation based Multi-tAsk Learning (NORMAL) method to alleviate this issue by modeling task-specific feature transformations from the perspective of dynamic flows built on the Neural Ordinary Differential Equation (NODE). Specifically, the proposed NORMAL model designs a time-aware neural ODE block to learn task-specific time information, which determines task positions of feature transformations in the dynamic flow, in NODE automatically via gradient descent methods. In this way, the proposed NORMAL model handles the problem of competing shared parameters by learning task positions. Moreover, the learned task positions can be used to measure the relevance among different tasks. Extensive experiments show that the proposed NORMAL model outperforms state-of-the-art MTL models.

1 Introduction

Multi-Task Learning (MTL) [Caruana, 1997; Zhang and Yang, 2022] is a paradigm that aims to learn one single model that can learn from several tasks simultaneously. As deep learning models are becoming larger and larger to solve complex problems, MTL becomes attractive since by sharing parameters across all the tasks and training all the tasks jointly, deep MTL models can reduce both the number of parameters and the training time.

*Corresponding author.

Among all the architectures for deep MTL, the Hard Parameter Sharing (HPS) architecture, which typically shares one feature extractor among tasks and after that has a task-specific head for each task, is the earliest and the most used one. Though it is simple, several works [Bartlett and Mendelson, 2002; Swersky *et al.*, 2013; Maurer *et al.*, 2016; Zamir *et al.*, 2018] point out that the HPS architecture is effective to improve the performance of each task. However, due to the use of a shared feature extractor to obtain a shared feature representation among tasks, the HPS architecture often faces the problem of competing for shared parameters among tasks during the training process, specifically in the form of gradient conflict which often leads to performance degradation for some tasks [Yu *et al.*, 2020; Liu *et al.*, 2021b]. To alleviate this problem, based on the HPS architecture, some recent studies [Chen *et al.*, 2018c; Sener and Koltun, 2018; Yu *et al.*, 2020; Liu *et al.*, 2021b; Liu *et al.*, 2021a; Navon *et al.*, 2022] propose loss weighting and gradient manipulation methods to help model training. Meanwhile, some works [Kumar and Daume III, 2012; Yao *et al.*, 2019] propose task grouping methods to mitigate the competition between tasks by combining more relevant tasks together to learn an HPS model. These methods require a lot of (pre-)grouping computation and increase the total model size.

Different from previous studies, in this paper, we study this problem from another perspective of the dynamic flow whose velocity is defined by a uniform function [Fleischer and Tardos, 1998] and propose a Neural Ordinal diffeRential equation based Multi-tAsk Learning (**NORMAL**) method. In the proposed NORMAL method, feature transformations of different tasks, which are placed after the shared feature extractor in the HPS architecture, are assumed to follow a dynamic flow and such task-specific feature transformations for different tasks could be modeled as different time points, which are called task positions, in a Neural Ordinary Differential Equation (NODE or Neural ODE) [Chen *et al.*, 2018b]. Different from NODEs, the task positions of different feature transformations in the dynamic flow, corresponding to the given time information in NODEs, are unknown, and the proposed NORMAL method utilizes a time-aware neural ODE block to learn task positions automatically via gradient descent meth-

ods. Empirically, extensive experiments demonstrate that the proposed NORMAL method outperforms state-of-the-art methods on benchmark datasets. Moreover, the learned task positions can reflect the task relations, which verifies the reasonableness of the learned task positions.

The main contributions of this work are three-fold.

- We are the first to model feature transformations in MTL from the perspective of dynamic flow and propose the NORMAL method to learn task positions that represent the task-specific feature transformations in the dynamic flow.
- The NORMAL method outperforms state-of-the-art methods on four benchmark datasets, including the Office-31, Office-Home, NYUv2, and CelebA datasets.
- The task positions learned by the NORMAL method can be used to evaluate the relevance of different tasks, which could improve the interpretability of the proposed NORMAL method.

2 Preliminary

In this section, we briefly introduce MTL as well as the first-order and second-order NODEs.

Multi-Task Learning. Given m learning tasks $\{\mathcal{T}_i\}_{i=1}^m$, task i has its corresponding dataset $\mathcal{D}_i$. Then the MTL model usually contains two parts of parameters: task-shared parameters θ and task-specific parameters $\{\phi_i\}_{i=1}^m$. The feature extractor $f_\theta(x) : \mathcal{X} \to \mathbb{R}^q$, which maps a sample $x \in \mathcal{X}$ into a q-dimensional feature space, is parameterized by task-shared parameters θ. Then, the i-th task-specific output module parameterized by task-specific parameters ϕ_i outputs the prediction as $h_{\phi_i}(f_\theta(x))$. Let $\mathcal{L}_i(\cdot,\cdot)$ denote the loss function for task i (e.g., the cross-entropy loss for classification tasks). MTL aims to learn all the parameters (i.e., $\theta, \phi_1, \phi_2, ..., \phi_m$) by minimizing the total loss as

$$\mathcal{L} = \frac{1}{m}\sum_{i=1}^{m}\frac{1}{n_i}\sum_{j=1}^{n_i}\mathcal{L}_i(y_i^j, h_{\phi_i}(f_\theta(x_i^j))), \tag{1}$$

where n_i denotes the number of samples for task i, x_i^j denotes the jth sample in task i, and y_i^j denotes the label of x_i^j. Built on problem (1), some works [Kendall *et al.*, 2018; Liu *et al.*, 2021b] design or learn task weighting on task losses, some works [Chen *et al.*, 2018c; Sener and Koltun, 2018; Yu *et al.*, 2020; Liu *et al.*, 2021b; Liu *et al.*, 2021a; Navon *et al.*, 2022] manipulate the gradient to alleviate the gradient conflicting issue, and some works [Kumar and Daume III, 2012; Yao *et al.*, 2019] identify task grouping.

First-order Neural ODEs. First-order NODEs [Chen *et al.*, 2018b] are proposed recently to model deep neural networks with continuous depths. NODEs model the dynamic of hidden features $z(t) \in \mathbb{R}^n$ via first-order Ordinary Differential Equations (ODEs), which is parameterized by a neural network $g(z(t), t, \varphi) \in \mathbb{R}^n$ with learnable parameters φ, i.e.,

$$\frac{dz(t)}{dt} = g(z(t), t; \varphi). \tag{2}$$

For a given initial value $z(t_0)$, NODEs obtain the output at time t with a black-box numerical ODE solver as

$$\begin{aligned} z(t) &= z(t_0) + \int_{t_0}^{t} g(z(s), s; \varphi)ds \\ &= \text{ODEsolver}(z(t_0), g, t_0, t; \varphi). \end{aligned}$$

The main technical difficulty in training such NODEs is how to do the back-propagation through the ODE solver efficiently. In [Chen *et al.*, 2018b], an adjoint sensitivity method is proposed to solve this issue. This method has a low memory cost, and can explicitly control numerical errors.

Second-order Neural ODEs. As the first-order NODEs are easy to suffer from unstable training, slow speed, and lack of highly expressive power, there are many works [Dupont *et al.*, 2019; da Silva and Gazeau, 2020; Xia *et al.*, 2021] to improve first-order NODEs. Among them, the Heavy Ball NODE (HBNODE) [Xia *et al.*, 2021] is more accurate and stable, and it is formulated as

$$\frac{d^2z(t)}{dt^2} + \gamma\frac{dz(t)}{dt} + g(z(t), t) = 0. \tag{3}$$

where $\gamma \geq 0$ is a damping factor and $g(\cdot,\cdot)$ represents a continuous function. In practice, γ can be treated as a hyperparameter or a learnable parameter, and $g(\cdot,\cdot)$ can be parameterized by a neural network. Eq. (3) can be reformulated as a first-order NODE system as

$$\frac{dz(t)}{dt} = -q(t),\ \frac{dq(t)}{dt} = -\gamma q(t) + g(z(t), t), \tag{4}$$

where $q(t) \in \mathbb{R}^n$ is a momentum function, and the starting point $q(0)$ is computed as $q(0) = -dz(t)/dt\ |_{t=0}$, which represents the initial velocity of $z(t)$. Following the idea of skip connection, one extra term $\xi z(t)$ is added to the second-order ODE system in HBNODE and the final formulation is

$$\begin{cases} \dfrac{dz(t)}{dt} = -q(t), \\ \dfrac{dq(t)}{dt} = -\gamma q(t) + g(z(t), t) + \xi z(t). \end{cases} \tag{5}$$

3 NORMAL

In this section, we will introduce the proposed NORMAL method.

3.1 The Entire Model

To mitigate competition for shared parameters by learning task-specific feature representations while retaining the benefits of MTL to learn feature representations, we treat feature transformations of different tasks as points embedded in a dynamic flow of transformations and use a NODE to model smoothly varying embeddings. So different task positions on the dynamic flow can be converted into outputs at different times on the NODE.

The NORMAL model consists of a shared feature extractor f_θ which is parameterized by θ, a task-shared dynamic flow modeled by a time-aware neural ODE block Q_φ which is parameterized by φ, and will be introduced in the next section,

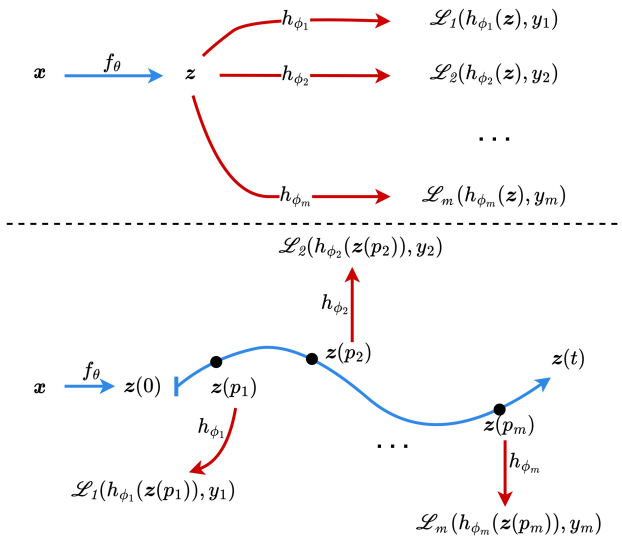

Figure 1: Comparison between the HPS-based MTL model (top) and the proposed NORMAL model (bottom). The HPS-based MTL model maps inputs into a shared intermediate representation. The NORMAL method uses task-specific feature transformation which is modeled by task positions in NODE to map inputs into task-specific feature representations. The blue color indicates task-shared components, and the red color denotes task-specific components.

learnable task positions $\{p_i\}$, and task-specific heads $\{h_{\phi_i}\}$. Here Q_φ is to model feature transformations from different tasks in a dynamic flow. Thus, as shown in Figure 1, for a sample in the ith task, the NORMAL model first obtains a hidden representation via f_θ, then moves to task position p_i over Q_φ to learn a feature transformation to obtain a feature representation with task specificity, and finally feed into h_{ϕ_i} to obtain the final output.

Mathematically, the objective function of the NORMAL model is formulated as

$$\min_{\Theta,\{p_i\}} \frac{1}{m}\sum_{i=1}^{m}\frac{1}{n_i}\sum_{j=1}^{n_i}\mathcal{L}_i(y_i^j, h_{\phi_i}(Q_\varphi(f_\theta(x_i^j), p_i))), \quad (6)$$

where Θ denotes all the network parameters, including φ, θ, and $\{\phi_i\}_{i=1}^m$, and $Q_\varphi(\cdot, p_i)$ denotes the output of the time-aware neural ODE block at task position p_i. Thus, in terms of notations of NODE as introduced in the previous section, we have $Q_\varphi(f_\theta(x_i), p_i) = z(p_i)$, where $z(0) = f_\theta(x_i)$.

3.2 Time-aware Neural ODE Block

In the time-aware neural ODE block, $f_\theta(x_i^j)$ extracted by the shared feature extractor is considered as the state at initial time/position 0 in the dynamic flow, and if p_i is known, then task-specific feature transformations could be learned. However, $\{p_i\}$ are usually unknown, and we aim to learn them.

Though first-order NODEs easily model dynamic flow, due to their instability, using them to implement Q_φ often leads to poor performance. Therefore, some second-order NODE (e.g., HBNODE) is used to build this block. Specifically,

Algorithm 1 The NORMAL model.

Input: training data and learning rates μ, η
Output: Task-shared parameters θ, φ, task-specific parameters $\{\phi_i\}$, $\{p_i\}$

1: **for** $k = 1$ **to** K **do**
2: Compute and save outputs of the time-aware neural ODE block for each task: $z(p_i)$ and $q(p_i)$;
3: Compute total loss $\mathcal{L}$ according to Eq. (6);
4: Compute the gradient d_{p_i} with respect to p_i according to Eq. (7);
5: Compute the gradient $\nabla_\Theta \mathcal{L}$ with respect to $\{\theta, \{\phi_t\}, \varphi\}$;
6: Update Θ as $\Theta := \Theta - \mu\nabla_\Theta\mathcal{L}$;
7: Update p_i as $p_i := p_i - \eta d_{p_i}$;
8: **end for**

based on Eq. (5), by using $f_\theta(x_i^j)$ as the initial value $z(0)$ of $z(t)$ for task i, we have

$$\begin{aligned} Q_\varphi(f_\theta(x_i^j), p_i) &= f_\theta(x_i^j) + \int_0^{p_i} -q(t)dt \\ &= f_\theta(x_i^j) - \int_0^{p_i}\left(q(0) + \int_0^t \frac{dq(l)}{dl}dl\right)dt. \end{aligned}$$

where $\frac{dq(l)}{dl} = -\gamma q(l) + g(z(l), l) + \xi z(l)$ and a mapping function $u(z) : \mathbb{R}^n \to \mathbb{R}^n$ maps $f_\theta(x_i^j)$ to the initial velocity $q(0)$. The initial velocity mapping $u(z; \varphi_v)$ and the ODE function $g(z, t; \varphi_o)$ are parameterized by φ_v and φ_o, respectively. Thus, the time-aware neural ODE block Q_φ is formulated as

$$\begin{aligned} Q_\varphi(f_\theta(x_i^j), p_i) = & f_\theta(x_i^j) - \int_0^{p_i}\Big(u(f_\theta(x_i^j); \varphi_v) + \\ & \int_0^t\big(-\gamma q(l) + g(z(l), l; \varphi_o) + \xi z(l)dl\big)\Big)dt. \end{aligned}$$

where $\gamma > 0$ is treated a learnable parameter and ξ is treated as a hyperparameter to be tuned. To guarantee the positiveness of γ, we reparameterize it as $\gamma = \text{sigmoid}(\omega)$, where ω is a learnable parameter. For simplicity, we denote these parameters by $\varphi = \{\varphi_v, \varphi_o, \omega\}$.

By using the block presented above, we can now calculate $z(t)$ for any given initial value $z(0) = f_\theta(x_i^j)$ and p_i. Existing studies on NODEs assume that p_i is available before training. In the proposed NORMAL method, if a common p_i is used for all the tasks, the NODE could be absorbed into $f_\theta(\cdot)$ and different tasks could have identical feature representations, which degenerates to the HPS architecture. If different tasks use different fixed p_i, setting them is too inefficient and does not have good performance according to our empirical observations. Therefore, in the NORMAL method, to achieve high expressive power in learned feature representations and low manual costs, we learn $\{p_i\}$ for all the tasks, which will be detailed in the next section.

3.3 Optimization

To learn parameters in the time-aware neural ODE block, we apply the adjoint sensitivity method, which can signifi-

cantly reduce the memory cost during calculating the gradient. However, we cannot use auto differentiation to update $\{p_i\}$ since current mainstream frameworks (e.g., Tensorflow and Pytorch) do not support automatically computing the gradient for task positions $\{p_i\}$ in NODEs, and we need to manually compute the gradient with respect to $\{p_i\}$. Specifically, for task i, the average loss L_i is defined as

$$L_i = \frac{1}{n_i}\sum_{j=1}^{n_i}\mathcal{L}_i(y_i^j, h_{\phi_i}(z(p_i)))).$$

where $z(p_i) = Q_\varphi(f_\theta(x_i^j), p_i)$.

Based on the chain rule, we compute the gradient with respect to p_i as

$$d_{p_i} = \left.\frac{dL_i}{dt}\right|_{t=p_i} = \frac{dL_i}{dz(t)}\left.\frac{dz(t)}{dt}\right|_{t=p_i} = -\frac{dL_i}{dz(p_i)}q(p_i). \quad (7)$$

In Eq. (7), $q(p_i)$ denotes the output of the momentum function at time p_i, which can be saved in the forward propagation process. Thus, we need to calculate the gradient of the loss L_i with respect to the output of the time-aware neural ODE block at time p_i. This does not require us to backpropagate the entire model, so it is not computationally expensive. Therefore, we can use d_{p_i} to update p_i as $p_i := p_i - \eta d_{p_i}$, where η represents the step size.

The gradients of other model parameters in the NORMAL method can be computed by auto differentiation and stochastic gradient descent methods can be used to update them. In the NORMAL method, we can update all the learnable parameters jointly or alternatively. Algorithm 1 summarizes the training algorithm for the NORMAL method.

4 Related Work

Multi-Task Learning. Built on the HPS architecture, there are several loss weighting and gradient manipulation methods for MTL. For example, GradNorm [Chen *et al.*, 2018c] learns loss weights to balance the norms of the scaled gradients for different tasks. PCGrad [Yu *et al.*, 2020] avoids the gradient conflicting between each pair of tasks by projecting the gradient of one task onto the normal plane of that of the other task. IMTL [Liu *et al.*, 2021b] finds a descent direction that has equal projections on the gradient of each task. CAGrad [Liu *et al.*, 2021a] minimizes the maximum of the decreasing of task losses while enforcing the update direction to be close to the average gradient among tasks. Nash-MTL [Navon *et al.*, 2022] considers MTL as a bargaining game and finds a Nash bargaining solution. The proposed NORMAL method studies MTL from a new perspective of dynamic flow, which is different from previous works in MTL.

Neural Ordinary Differential Equation. NODEs [Chen *et al.*, 2018b] can learn from irregularly sampled data and are particularly suitable for learning complex dynamical systems. NODE-based methods have shown promising performance on a number of tasks including building normalizing flows [Finlay *et al.*, 2020], modeling continuous time data [Yildiz *et al.*, 2019], and generative models [Grathwohl *et al.*, 2019]. However, training NODEs on large datasets is not an easy task and often leads to poor performance. This is because the training process of NODE is very slow [Xia *et al.*, 2021], and NODE often fails to learn long-term dependencies in sequential data [Lechner and Hasani, 2020]. The HBNODE [Xia *et al.*, 2021] is based on second-order ODEs with a damping term, which can significantly accelerate the training process and provide a stable result.

5 Experiments

In this section, we empirically evaluate the proposed NORMAL method on four benchmark datasets, including Office-31 [Saenko *et al.*, 2010], Office-Home [Venkateswara *et al.*, 2017], NYUv2 [Silberman *et al.*, 2012], and CelebA [Liu *et al.*, 2015]. All experiments are performed on a single NVIDIA GeForce RTX 3090 GPU.

Baselines. Here, we compare the proposed method with state-of-the-art MTL methods, including EW that adopts an equal weight on training losses of different tasks, UW [Kendall *et al.*, 2018], GradNorm [Chen *et al.*, 2018c], MGDA [Sener and Koltun, 2018], PCGrad [Yu *et al.*, 2020], IMTL [Liu *et al.*, 2021b], CAGrad [Liu *et al.*, 2021a], and Nash-MTL [Navon *et al.*, 2022].

Evaluation metric. For the Office-31, Office-Home, and CelebA datasets where all the tasks are classification tasks, we report the classification accuracy on each task and/or the average classification accuracy over tasks. For the NYUv2 dataset which has three tasks: 13-class semantic segmentation, depth estimation, and surface normal prediction, by following [Maninis *et al.*, 2019], we use the average of the relative improvement of each task over the EW method as the evaluation metric, which is formulated as

$$\Delta_b = \frac{1}{m}\sum_{i=1}^{m}\frac{1}{N_i}\sum_{j=1}^{N_i}\frac{(-1)^{s_{i,j}}(M_{i,j}^b - M_{i,j}^{EW})}{M_{i,j}^{EW}},$$

where m denotes the number of tasks, N_i denotes the number of metrics for task i, $M_{i,j}^b$ denotes the performance of an MTL method b for the jth metric in task i, $M_{i,j}^{EW}$ is defined in the same way for the EW method, and $s_{i,j}$ is set to 1 if a lower value indicates better performance for the jth metric in task i and otherwise 0.

5.1 Results on Office-31 and Office-Home Datasets

Datasets. The **Office-31** dataset [Saenko *et al.*, 2010] includes images from three different sources: images downloaded from www.amazon.com (**A**mazon), images from digital SLR cameras (**D**slr), and images from webcams (**W**ebcam). It contains 31 categories for each source and a total of 4652 labeled images. The **Office-Home** dataset [Venkateswara *et al.*, 2017] includes images from four sources: artistic images (**Ar**), clip art (**Cl**), product images (**Pr**), and real-world images (**Rw**). It contains 65 categories for each source and a total of 15,500 labeled images. Under the multi-task learning setting, we treat each source as a separate task, so these two datasets can be used as a multi-task classification problem.

Method	Office-31				Office-Home				
	A	D	W	Avg	Ar	Cl	Pr	Rw	Avg
EW	84.67	98.09	98.70	93.82	64.77	79.05	90.11	80.44	78.59
UW	84.62	97.81	98.89	93.77	66.03	79.09	89.69	79.78	78.65
GradNorm	84.22	98.09	98.89	93.73	64.84	78.73	89.86	**80.58**	78.50
MGDA	78.69	98.09	98.70	91.83	65.40	75.05	89.76	79.96	77.54
PCGrad	84.67	97.81	98.70	93.73	65.27	78.37	90.08	79.89	78.40
IMTL	83.02	98.09	98.89	93.33	65.27	77.72	89.90	80.54	78.36
CAGrad	84.33	97.81	**99.07**	93.74	64.90	78.48	**90.47**	80.18	78.50
Nash-MTL	83.82	98.91	**99.07**	93.93	66.79	78.66	90.29	79.82	78.89
NORMAL	**86.32**	**99.18**	98.88	**94.80**	**69.26**	**80.39**	**90.47**	80.22	**80.08**

Table 1: Classification accuracy (%) of different methods on the **Office-31** and **Office-Home** datasets. Each experiment is repeated over 3 random seeds and the mean is reported. The best results for each task are shown in **bold**.

Method	Segmentation		Depth		Surface Normal					$\Delta\uparrow$
					Angle Distance		Within t°			
	mIoU↑	Pix Acc ↑	Abs Err ↓	Rel Err↓	Mean ↓	Median ↓	11.25 ↑	22.5 ↑	30 ↑	
EW	**0.4875**	0.7183	0.4179	0.1734	25.42	18.84	0.3243	0.5729	0.6845	0%
UW	0.4866	0.7165	**0.4085**	0.1711	25.42	18.77	0.3212	0.5703	0.6829	0.45%
GradNorm	0.4789	0.7106	0.4134	0.1686	25.40	18.61	0.3237	0.5733	0.6848	0.26%
MGDA	0.4138	0.6631	0.4416	0.1825	**24.33**	**17.48**	**0.3423**	**0.5975**	**0.7065**	-3.97%
PCGrad	0.4835	0.7155	0.4124	0.1718	25.40	18.66	0.3230	0.5726	0.6844	0.21%
IMTL	0.4769	0.7112	0.4141	0.1711	24.76	17.90	0.3355	0.5881	0.6978	0.89%
CAGrad	0.4777	0.7113	0.4128	**0.1676**	24.80	17.92	0.3356	0.5874	0.6973	1.29%
Nash-MTL	0.4764	0.7103	0.4155	0.1704	24.64	17.71	0.3409	0.5911	0.6999	1.12%
NORMAL	0.4857	**0.7184**	0.4113	0.1691	24.98	18.34	0.3352	0.5827	0.6923	**1.33%**

Table 2: Performance on three tasks (i.e. 13-class semantic segmentation, depth estimation, and surface normal prediction) in the **NYUv2** dataset. Each experiment is repeated over 3 random seeds and the mean is reported. The best results for each task are shown in **bold**.↑(↓) means that the higher (lower) the value, the better the performance.

Implementation Details. On both datasets, we use a ResNet-18 network pre-trained on the ImageNet dataset as f_θ, the Euler's method as the ODE solver, and a task-specific fully connected layer as the corresponding head for each task.

Implementation Details of Time-aware Neural ODE Blocks. The architectures of the initial velocity $u(z;\varphi_v)$ and ODE function $g(z,t;\varphi_o)$ are constructed as follows.

- Initial Velocity: $\rightarrow$ FC $\rightarrow$ LeakyReLU $\rightarrow$ FC $\rightarrow$
- ODE Function: $\rightarrow$ FC $\rightarrow$ LeakyReLU $\rightarrow$ FC $\rightarrow$

All the fully connected (FC) layers of both functions have a dimension of 512 for inputs and outputs.

Results. The results on the Office-31 and Office-Home datasets are shown in Table 1. We can see that on both datasets, the NORMAL method outperforms state-of-the-art baseline methods in terms of average classification accuracy. Compared with the unbalanced performance of several baseline methods on different tasks, the NORMAL method achieves a boost on almost all tasks over the EW method. For example, on the Office-31 dataset, the MGDA method performs well on the **D** and **W** tasks but performs very poorly on the **A**, which does not occur in the NORMAL method. This result demonstrates the advantage of the NORMAL method in that it can learn better feature representations for each task by learning task-specific feature transformations over dynamic flow. Moreover, compared with baselines, the proposed NORMAL method achieves the best result in some tasks, such as the best classification accuracy of 86.32% in task **A** for the Office-31 dataset and 69.26% classification accuracy in task **Ar** for the Office-Home dataset.

5.2 Results on the NYUv2 Dataset

Dataset. The **NYUv2** dataset [Silberman *et al.*, 2012] consists of video sequences of various indoor scenes recorded by RGB and Depth cameras in Microsoft Kinect. It contains 1,449 images with ground truth, where 795 images are for training and 654 images are for validation. This dataset has three tasks: 13-class semantic segmentation, depth estimation, and surface normal prediction.

Implementation Details. On the NYUv2 dataset, we use the DeepLabV3+ architecture [Chen *et al.*, 2018a] with HBN-ODE. Specifically, we use pre-trained Resnet-18 with dilated convolutions [Yu *et al.*, 2017] as the feature extractor shared by all tasks, the Euler's method as the ODE solver, and the Atrous Spatial Pyramid Pooling (**ASPP**) [Chen *et al.*, 2018a] as the task-specific header for each task.

Implementation Details of Time-aware Neural ODE Blocks. The architectures of the initial velocity $u(z;\varphi_v)$

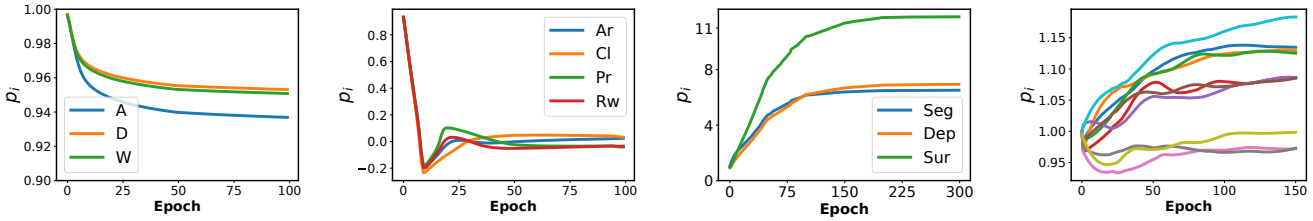

(a) Office-31 Dataset (b) Office-Home Dataset (c) NYUv2 Dataset (d) CelebA Dataset

Figure 2: Task positions $\{p_i\}$ throughout the training process on the four datasets.

and ODE function $g(z, t; \varphi_o)$ are constructed as follows.

- Initial Velocity: $\rightarrow$ Conv $\rightarrow$ LeakyReLU $\rightarrow$ Conv $\rightarrow$
- ODE Function: $\rightarrow$ Conv $\rightarrow$ LeakyReLU $\rightarrow$ Conv $\rightarrow$

The numbers of the input channel and output channel of the convolution layers of both functions are set to 512, the size of the kernel is 1, the stride size is 1, and the padding is 0.

Results. The results on the NYUv2 dataset are shown in Table 2. Overall, the proposed NORMAL method achieves good performance when compared with the state-of-the-art baseline methods. The MGDA method obtains the best results on all metrics of the surface normal prediction task, but performs poorly in the other two tasks, thus its overall performance is not so good. In contrast, The NORMAL method achieves relatively balanced performance on all the tasks, and hence its overall performance in terms of Δ exceeds all other methods. This illustrates the ability of the NORMAL method to effectively improve performance on all the tasks by finding task positions.

5.3 Results on CelebA Dataset

Dataset. The **CelebA** dataset [Liu *et al.*, 2015] includes a total of 202,599 face images and 40 face attribute annotations. In the multi-task learning setup, each face attribute is treated as a task. Thus, there are 40 classification tasks in this dataset.

Implementation Details. On the CelebA dataset, we use Resnet-18 with an average-pooling as the task-shared feature extractor f_θ, the Euler's method as our ODE solver, and a fully connected layer as the task-specific head for each task.

Implementation Details of Time-aware Neural ODE Blocks. The architectures of the initial velocity $u(z; \varphi_v)$ and ODE function $g(z, t; \varphi_o)$ are constructed as follows.

- Initial Velocity: $\rightarrow$ FC $\rightarrow$ LeakyReLU $\rightarrow$ FC $\rightarrow$
- ODE Function: $\rightarrow$ FC $\rightarrow$ LeakyReLU $\rightarrow$ FC $\rightarrow$

All fully connected layers of both functions have a dimension of 2048 for both inputs and outputs.

Results. According to the results shown in Table 3, we can see that the NORMAL method achieves the best average classification accuracy performance on the CelebA dataset, which again demonstrates the effectiveness of the NORMAL method.

Method	**Avg**
EW	90.78
UW	90.82
GradNorm	90.69
MGDA	90.40
PCGrad	90.93
IMTL	90.46
CAGrad	90.73
Nash-MTL	90.83
NORMAL	**91.00**

Table 3: Average classification accuracy (%) of different methods on the **CelebA** dataset with 40 tasks. Each experiment is repeated over 3 random seeds and the mean is reported. The best results are shown in **bold**.

5.4 Analysis on Learned Task Positions

In this section, we analyze the learned task positions $\{p_i\}$ to see why the NORMAL method achieves good performance on these datasets.

The training curves of all $\{p_i\}$ on the four benchmark datasets are shown in Figure 2, where due to the large number of tasks in the CelebA dataset, we randomly select a portion of the tasks for better illustration. According to Figure 2, we have two observations.

Firstly, the proposed NORMAL method does successfully learn task positions. Taking the training curves of $\{p_i\}$ on the NYUv2 dataset in Figure 2(c) as an example, we can see that its training trajectory is very smooth and all task positions eventually converge to their own convergent points. We can also find similar results in Figures 2(a) and 2(b). In Figure 2(d), though the training trajectory is not as smooth as the other three datasets, the proposed NORMAL method can still differentiate tasks and find their own task positions.

Secondly, $\{p_i\}$ learned by the NORMAL method are able to reflect task relations. For example, according to Figures 2(a) and 2(b), the task positions in these two datasets converge to a very similar value. This result is consistent with the nature of the Office-31 and the Office-Home datasets in that different tasks in each dataset are semantically similar due to the shared label space among tasks. In Figure 2(c), we find that p_{sur} learned for the surface normal prediction task is different from p_{seg} and p_{dep} learned for the semantic segmentation and depth estimation tasks, which indicates that the

Setting	Office-31				Office-Home				
	A	D	W	Avg	Ar	Cl	Pr	Rw	Avg
Constant and identical $\{p_i\}$	84.62	98.36	98.89	93.95	61.35	75.37	87.75	75.28	74.94
Constant but different $\{p_i\}$	85.24	98.36	98.52	94.04	61.35	75.37	87.75	75.28	74.94
Different form of p_i: $p_i = e^{\nu_i}$	85.47	97.81	98.70	94.00	68.82	79.23	89.55	80.68	79.57
Using first-order NODE	84.79	98.36	98.89	94.01	65.27	77.57	88.98	76.97	77.45
Adding task-shared layers	83.87	97.81	98.15	93.28	58.13	73.28	85.06	72.43	72.22
Adding task-specific layers	83.87	97.81	97.59	93.09	60.34	74.50	87.25	74.31	74.10
NORMAL	86.32	99.18	98.88	94.80	69.26	80.39	90.47	80.22	80.08

Table 4: Ablation studies on the **Office-31** and **Office-Home** datasets in terms of the classification accuracy (%). Each experiment is repeated over 3 random seeds and the mean is reported.

surface normal prediction task is not so related to the other two tasks, and this observation matches some previous study [Sun *et al.*, 2021], which verifies that the learned $\{p_i\}$ can reflect task relations. In Figure 2(d), we can see that different tasks tend to form several groups based on learned task positions $\{p_i\}$. For example, some tasks (e.g., Sideburns and Wavy_Hair) have similar task positions as face attributes corresponding to those tasks are similar. Moreover, some tasks (e.g., Receding_ Hairline and 5_o_Clock_Shadow) have different task positions since face attributes corresponding to those tasks are totally different. Those results show that the learned task positions could help identify task clusters.

In summary, the proposed NORMAL method could learn meaningful task positions that can reveal task relations.

5.5 Ablation Studies

In this section, we conduct ablation studies on the Office-31 and Office-Home datasets to answer several questions which are placed at the beginning of the following paragraphs.

Are the learned task positions advantageous compared with fixed task positions? We try to use a fixed parameter p shared by all tasks and use task-specific fixed parameters $\{p_i\}$ for different tasks. For the former setting, we use $p = 1$. In the latter setting, for the Office-31 dataset, we try to set task positions of the three tasks to each permutation of a set $\{1, 1.25, 1.5\}$ and select the best performed one, and for the Office-Home dataset, the set to generate task positions is $\{1, 1.25, 1.5, 1.75\}$. According to the results shown in Table 4, the performance of the two settings for task positions is inferior to the learning of task positions in the proposed NORMAL method, which demonstrates the effectiveness of the learning strategy for task positions in the NORMAL method.

How do different forms of learning task positions impact the performance? Here we try positive task positions and parameterize task positions $\{p_i\}$ as $p_i = e^{\nu_i}$. As shown in Table 4, the model learned here is inferior to that of the NORMAL model without any constraint on task positions by 0.80% and 0.51% on the Office-31 and Office-Home datasets, respectively, which shows that learning task positions without the positive requirement may be better. Based on Tables 1 and 4, this variant to learn positive task positions still performs better than baseline methods, which again verifies the effectiveness of the NORMAL method.

How do different NODE algorithms impact the performance? The NORMAL method uses a second-order ODE method but not first-order NODEs. Here we explore whether different methods in the NODE family impact the performance of the NORMAL method. We evaluate the performance of the NORMAL method using the first-order NODE [Chen *et al.*, 2018b]. According to results shown in Tables 1 and 4, we can see that on the Office-Home dataset, the performance of the NORMAL method using the first-order NODE method is worse than the NORMAL method and baseline methods. Some possible reasons are that first-order NODEs usually cannot be trained stably and that second-order NODEs are more expressive. For the Office-31 dataset, the NORMAL method with the first-order NODE performs slightly worse than the NORMAL method but slightly better than the baseline methods. One possible reason is that the Office-31 dataset is easier than the Office-Home dataset. In summary, second-order NODE methods are preferred to be used in the NORMAL method.

Does the enhancement of the NORMAL method result from the addition of certain parameters? The time-aware neural ODE block in the NORMAL method introduces a small number of parameters, which are almost negligible compared to other model parameters. We aim to investigate whether such an increasing number of parameters brings performance gain. Therefore, we experiment to add task-shared layers in f_θ and task-specific layers in $\{h_{\phi_i}\}$, respectively, to match with the number of parameters in NORMAL method, and show results in Table 4. According to the results, we can see that the introduction of additional layers does not bring a performance improvement, and even lead to performance degradation. One possible reason could be the overfitting issue. Through this experiment, we can see that the performance of the NORMAL method is attributed from the entire model design but not the introduction of more parameters.

6 Conclusion

In this work, we propose the NORMAL algorithm to model multiple learning tasks from the perspective of dynamic flow. By learning the task positions in the NODE, the NORMAL method can model the task relations in terms of the relative task positions. Experiments on benchmark datasets demonstrate the effectiveness of the proposed NORMAL method.

Acknowledgments

This work is supported by NSFC key grant under grant no. 62136005, NSFC general grant under grant no. 62076118, and Shenzhen fundamental research program JCYJ20210324105000003.

Contribution Statement

Feiyang Ye and Xuehao Wang contributed equally to this work.

References

[Bartlett and Mendelson, 2002] Peter L Bartlett and Shahar Mendelson. Rademacher and gaussian complexities: Risk bounds and structural results. *Journal of Machine Learning Research*, 3(Nov):463–482, 2002.

[Caruana, 1997] Rich Caruana. Multitask learning. *Machine learning*, 28(1):41–75, 1997.

[Chen *et al.*, 2018a] Liang-Chieh Chen, Yukun Zhu, George Papandreou, Florian Schroff, and Hartwig Adam. Encoder-decoder with atrous separable convolution for semantic image segmentation. In *Proceedings of the European conference on computer vision (ECCV)*, pages 801–818, 2018.

[Chen *et al.*, 2018b] Ricky TQ Chen, Yulia Rubanova, Jesse Bettencourt, and David K Duvenaud. Neural ordinary differential equations. *Advances in neural information processing systems*, 31, 2018.

[Chen *et al.*, 2018c] Zhao Chen, Vijay Badrinarayanan, Chen-Yu Lee, and Andrew Rabinovich. Gradnorm: Gradient normalization for adaptive loss balancing in deep multitask networks. In *International conference on machine learning*, pages 794–803. PMLR, 2018.

[da Silva and Gazeau, 2020] André Belotto da Silva and Maxime Gazeau. A general system of differential equations to model first-order adaptive algorithms. *J. Mach. Learn. Res.*, 21, 2020.

[Dupont *et al.*, 2019] Emilien Dupont, Arnaud Doucet, and Yee Whye Teh. Augmented neural odes. *Advances in Neural Information Processing Systems*, 32, 2019.

[Finlay *et al.*, 2020] Chris Finlay, Jörn-Henrik Jacobsen, Levon Nurbekyan, and Adam Oberman. How to train your neural ode: the world of jacobian and kinetic regularization. In *International conference on machine learning*, pages 3154–3164. PMLR, 2020.

[Fleischer and Tardos, 1998] Lisa Fleischer and Éva Tardos. Efficient continuous-time dynamic network flow algorithms. *Operations Research Letters*, 23(3-5):71–80, 1998.

[Grathwohl *et al.*, 2019] Will Grathwohl, Ricky TQ Chen, Jesse Bettencourt, and David Duvenaud. Scalable reversible generative models with free-form continuous dynamics. In *International Conference on Learning Representations*, 2019.

[Kendall *et al.*, 2018] Alex Kendall, Yarin Gal, and Roberto Cipolla. Multi-task learning using uncertainty to weigh losses for scene geometry and semantics. In *Proceedings of the IEEE conference on computer vision and pattern recognition*, pages 7482–7491, 2018.

[Kumar and Daume III, 2012] Abhishek Kumar and Hal Daume III. Learning task grouping and overlap in multi-task learning. *arXiv preprint arXiv:1206.6417*, 2012.

[Lechner and Hasani, 2020] Mathias Lechner and Ramin Hasani. Learning long-term dependencies in irregularly-sampled time series. *arXiv preprint arXiv:2006.04418*, 2020.

[Liu *et al.*, 2015] Ziwei Liu, Ping Luo, Xiaogang Wang, and Xiaoou Tang. Deep learning face attributes in the wild. In *Proceedings of the IEEE international conference on computer vision*, pages 3730–3738, 2015.

[Liu *et al.*, 2021a] Bo Liu, Xingchao Liu, Xiaojie Jin, Peter Stone, and Qiang Liu. Conflict-averse gradient descent for multi-task learning. *Advances in Neural Information Processing Systems*, 34:18878–18890, 2021.

[Liu *et al.*, 2021b] Liyang Liu, Yi Li, Zhanghui Kuang, J Xue, Yimin Chen, Wenming Yang, Qingmin Liao, and Wayne Zhang. Towards impartial multi-task learning. ICLR, 2021.

[Maninis *et al.*, 2019] Kevis-Kokitsi Maninis, Ilija Radosavovic, and Iasonas Kokkinos. Attentive single-tasking of multiple tasks. In *Proceedings of the IEEE/CVF Conference on Computer Vision and Pattern Recognition*, pages 1851–1860, 2019.

[Maurer *et al.*, 2016] Andreas Maurer, Massimiliano Pontil, and Bernardino Romera-Paredes. The benefit of multitask representation learning. *Journal of Machine Learning Research*, 17(81):1–32, 2016.

[Navon *et al.*, 2022] Aviv Navon, Aviv Shamsian, Idan Achituve, Haggai Maron, Kenji Kawaguchi, Gal Chechik, and Ethan Fetaya. Multi-task learning as a bargaining game. *arXiv preprint arXiv:2202.01017*, 2022.

[Saenko *et al.*, 2010] Kate Saenko, Brian Kulis, Mario Fritz, and Trevor Darrell. Adapting visual category models to new domains. In *European conference on computer vision*, pages 213–226. Springer, 2010.

[Sener and Koltun, 2018] Ozan Sener and Vladlen Koltun. Multi-task learning as multi-objective optimization. *Advances in neural information processing systems*, 31, 2018.

[Silberman *et al.*, 2012] Nathan Silberman, Derek Hoiem, Pushmeet Kohli, and Rob Fergus. Indoor segmentation and support inference from rgbd images. In *European conference on computer vision*, pages 746–760. Springer, 2012.

[Sun *et al.*, 2021] Guolei Sun, Thomas Probst, Danda Pani Paudel, Nikola Popović, Menelaos Kanakis, Jagruti Patel, Dengxin Dai, and Luc Van Gool. Task switching network for multi-task learning. In *Proceedings of the*

IEEE/CVF International Conference on Computer Vision, pages 8291–8300, 2021.

[Swersky *et al.*, 2013] Kevin Swersky, Jasper Snoek, and Ryan P Adams. Multi-task Bayesian optimization. 2013.

[Venkateswara *et al.*, 2017] Hemanth Venkateswara, Jose Eusebio, Shayok Chakraborty, and Sethuraman Panchanathan. Deep hashing network for unsupervised domain adaptation. In *Proceedings of the IEEE conference on computer vision and pattern recognition*, pages 5018–5027, 2017.

[Xia *et al.*, 2021] Hedi Xia, Vai Suliafu, Hangjie Ji, Tan Nguyen, Andrea Bertozzi, Stanley Osher, and Bao Wang. Heavy ball neural ordinary differential equations. *Advances in Neural Information Processing Systems*, 34:18646–18659, 2021.

[Yao *et al.*, 2019] Yaqiang Yao, Jie Cao, and Huanhuan Chen. Robust task grouping with representative tasks for clustered multi-task learning. In *Proceedings of the 25th ACM SIGKDD International Conference on Knowledge Discovery & Data Mining*, pages 1408–1417, 2019.

[Yildiz *et al.*, 2019] Cagatay Yildiz, Markus Heinonen, and Harri Lahdesmaki. Ode2vae: Deep generative second order odes with bayesian neural networks. *Advances in Neural Information Processing Systems*, 32, 2019.

[Yu *et al.*, 2017] Fisher Yu, Vladlen Koltun, and Thomas Funkhouser. Dilated residual networks. In *Proceedings of the IEEE conference on computer vision and pattern recognition*, pages 472–480, 2017.

[Yu *et al.*, 2020] Tianhe Yu, Saurabh Kumar, Abhishek Gupta, Sergey Levine, Karol Hausman, and Chelsea Finn. Gradient surgery for multi-task learning. *Advances in Neural Information Processing Systems*, 33:5824–5836, 2020.

[Zamir *et al.*, 2018] Amir R Zamir, Alexander Sax, William Shen, Leonidas J Guibas, Jitendra Malik, and Silvio Savarese. Taskonomy: Disentangling task transfer learning. In *Proceedings of the IEEE conference on computer vision and pattern recognition*, pages 3712–3722, 2018.

[Zhang and Yang, 2022] Yu Zhang and Qiang Yang. A survey on multi-task learning. *IEEE Transactions on Knowledge and Data Engineering*, 34(12):5586–5609, 2022.